PHYSICAL REVIEW A **107**, L020801 (2023)

Letter

Unexpected dipole instabilities in small molecules after ultrafast XUV irradiation

P.-G. Reinhard,[1] D. Dundas,[2] P. M. Dinh,[3] M. Vincendon,[3] and E. Suraud[3]

[1] *Institut für Theoretische Physik, Universität Erlangen, Staudtstraße 7, Erlangen 91058, Germany*
[2] *School of Mathematics and Physics, Queen's University Belfast BT7 1NN, United Kingdom*
[3] *Laboratoire de Physique Théorique, Université de Toulouse, CNRS, UPS, Toulouse 31062, France*

(Received 19 May 2022; revised 10 October 2022; accepted 30 January 2023; published 17 February 2023)

We investigate the depletion of deep-lying single-electron states in the N_2 dimer under the influence of very short extreme-ultraviolet (XUV) pulses. We find, first, a marked occupation inversion for a certain window of XUV energies around 50 eV, where depletion of the deepest bound valence electron state is much larger than for any other state, and second, that this occupation inversion drives a dipole instability, i.e., a spontaneous reappearance of the dipole signal long after the laser pulse is over and the initial dipole oscillations have died out. As a tool for this study, we use time-dependent density functional theory with a self-interaction correction solved on a coordinate-space grid with absorbing boundary conditions. Key observables are state-specific electron emission (depletion) and photoelectron spectra (PES). The dipole instability generates additional electron emission, leading to a specific low-energy structure in PES, a signal which could be used to identify the dipole instability experimentally. The here reported dedicated depletion of a deep lying electron state by a well-tuned XUV pulse has also been found in other atoms and molecules. It provides a practicable realization of an instantaneously produced deep hole state, a situation which is often assumed ad hoc in numerous theoretical studies of energetic ultrafast processes. Moreover, the identification of the subsequent dipole instability by PES will allow one to study basic decay channels of hole states in detail.

DOI: 10.1103/PhysRevA.107.L020801

With the advent of ultrashort laser pulses in the extreme-ultraviolet (XUV) to X-ray frequency regime, attoscience has become a dynamically growing field over the last two decades [1]. The short pulse durations and the great flexibility in shaping pulses nourish hope for time-resolved measurements down to the electronic timescale [2]. The typically high photon energies extend electron excitations to deeper-lying states often down to core states. This can trigger various relaxation processes such as Auger decays [3], interatomic (or intermolecular) Coulomb decays [4], charge migration in covalent molecules [5,6], or giant autoionization resonance in high harmonic generation [7,8]. A fully detailed theoretical treatment of ultrafast excitation from the ground state to high-energy configurations remains highly demanding [9]. One thus often ignores the detailed excitation process by assuming that an attosecond XUV pulse instantaneously removes a bound electron [10,11]. This considerably simplifies the picture, since the excitation process is not considered explicitly and one can choose at will where the hole is created. Such an excitation model is thus routinely used to explore the dynamics of charge migration and charge transfer in molecular systems [12–19].

Here we take a closer look at the detailed excitation process induced by such a short XUV pulse. We simulate the full dynamical interaction of an ultrashort XUV pulse with a multielectronic system, and the electronic emission thereof, using time-dependent density functional theory (TDDFT) [20]. Thanks to a pseudopotential with frozen cores [21], we only consider valence electrons and focus on the depletion of the lowest occupied valence state, easily attainable with an XUV laser. Indeed low-frequency pulses skim electrons from the Fermi surface, while deeper-lying electrons come increasingly into play with increasing pulse frequency [22–24]. One might expect an equidistribution of depletion over all valence states, as observed in Na clusters [22,23] and C_{60} [24]. However, when considering ultrafast pulses in the few-femtosecond regime, we observe in covalent molecules an ionization mechanism very close to the creation of an instantaneous deep hole. A remarkable consequence is that this excitation leads to a dipole instability, with a delayed reappearance of the dipole signal well after the pulse is over and the dipole signal has died out. This instability leaves as an experimentally accessible footprint a low-energy peak in photoelectron spectra. We only consider here the simple N_2 molecule, but we found similar behavior in other small molecules such as acetylene. Additionally, our results are robust when including ionic motion and incoherent electronic dynamical correlations within a relaxation time approximation (RTA) [25]. This partly answers the question of the validity of time-dependent local density approximation (TDLDA) for such ultrafast setups.

We describe the electrons with the widely used TDDFT [20], at the level of the local density approximation (LDA) [26], using the functional of Ref. [27]. The single-particle (s.p.) wave functions are discretized on a real-space grid. The dynamical treatment of ionization requires realistic s.p. energies, particularly for the highest-occupied molecular orbital (HOMO). We thus add a self-interaction correction (SIC) [28], actually the simple and efficient average-density SIC (ADSIC) [29–32]. Electron emission is evaluated through absorbing boundary conditions via a mask function [33,34]. The coupling between electrons and ions is described using Goedecker-type pseudopotentials [21]. The ionic positions are kept frozen since the time scale of the electronic processes considered is very short. We have also performed calculations including electronic dynamical correlations at the level of the RTA [25,35,36]. As our test case will be N_2, which is an axially symmetric system, we employ here the two-dimensional (2D) axial version of the general code quantum dissipative dynamics (QDD) [36]. It allows us to scan a larger Hilbert space for the (initially unoccupied) states used in RTA dynamics [25,36]. Wave functions and fields are represented on a 2D axial grid with a grid spacing of 0.25 a_0: 301 grid points in the axial (z) direction, and 151 in the radial direction. The distance between the ions is taken as the minimum of the Born-Oppenheimer surface, which is 2.02 a_0 for our setup (pseudopotential and ADSIC). The stationary electronic state is computed using an accelerated gradient method, and the time-dependent Kohn-Sham equations are propagated using a time-splitting technique [36,37] with a time step of 0.0048 fs.

We will consider three observables. The first one is the time evolution of the dipole moment along laser polarization/molecular axis z: $D(t) = \int d^3\mathbf{r}\, ez\,\varrho(\mathbf{r})$. The single electron density is computed as $\varrho(\mathbf{r}) = \sum_\alpha w_\alpha(t)|\varphi_\alpha(\mathbf{r},t)|^2$ where $\varphi_\alpha(\mathbf{r},t)$ is the time-dependent s.p. wave function of state α and $w_\alpha(t)$ its occupation number. The summation here runs on all computed states. At LDA level, only occupied states are treated, and for these we have $w_\alpha = 1$ and independent of time. At RTA level, the w_α's become fractional and time dependent [25,36]. The dipole signal, recorded from initializing the dynamics with a small kick, provides the optical response of the system by spectral analysis [38].

The second observable is the electron content n_α per s.p. wave function, and the associated depletion $\bar{n}_\alpha$:

$$n_\alpha(t) = w_\alpha \int d^3\mathbf{r}\,|\varphi_\alpha(\mathbf{r},t)|^2, \quad \bar{n}_\alpha(t) = 1 - n_\alpha(t). \tag{1}$$

The total number of escaped electrons is $N_{\rm esc}(t) = \sum_\alpha \bar{n}_\alpha(t) = N - \sum_\alpha n_\alpha(t)$, where N is the initial number of computed electrons (10 for N_2).

Lastly, we analyze the electronic emission dynamics through photoelectron spectra (PES). At several measuring points shortly before the absorbing boundaries begin, we record the time evolution of each s.p. wave function and finally Fourier transform them to the frequency domain. This provides the spectrum of kinetic energies of the escaping electrons, that is, the PES [39–41]. In strong fields an additional phase correction has to be added [42].

The system is excited by an XUV pulse modeled as a classical (coherent) photon field linearly polarized along the symmetry axis z. The corresponding potential reads

$$V_{\rm pulse} = eE_0 z\, f(t) \cos[\omega_{\rm XUV}(t - T_{\rm pulse})] \tag{2a}$$

$$f(t) = \begin{cases} \sin^2\left(\pi \frac{t}{2T_{\rm pulse}}\right) & t \in \{0,\ 2T_{\rm pulse}\} \\ 0 & \text{otherwise.} \end{cases} \tag{2b}$$

The pulse parameters are the frequency $\omega_{\rm XUV}$, the duration $T_{\rm pulse}$, and the field strength E_0 (intensity $I \propto E_0^2$). We use $T_{\rm pulse} = 1$ fs and, for a given $\omega_{\rm XUV}$, adjust $E_0 = 1.46\,(\omega_{\rm XUV}/{\rm eV})^{3/2}\,{\rm eV}/a_0$ [corresponding to intensity $I = 10^{14}\,(\omega_{\rm XUV}/{\rm eV})^3\,{\rm W/cm^2}$] so that the asymptotic total ionization $N_{\rm esc}$ is approximately 1 throughout. We chose that scaling to come close to the mechanism of instantaneous generation of a hole in the lowest valence state.

The electronic ground state of N_2 with its ten valence electrons is prepared by solving the static Kohn-Sham equations. The emerging occupied ground-state s.p. states, each doubly occupied, have the following energies: $\varepsilon_{2\Sigma_g} = -32.5$ eV, $\varepsilon_{2\Sigma_u} = -18.6$ eV, $\varepsilon_{2\Pi_x} = \varepsilon_{2\Pi_y} = -17.7$ eV, $\varepsilon_{2\Pi_z} = \varepsilon_{\rm HOMO} = -15.1$ eV (= − ionization potential, IP). The experimental values are, for comparison, −37.3 eV, −18.6 eV, −16.6 eV, and −15.5 eV, respectively. This agrees well for the last three levels while leaving a 14% mismatch for the deepest one, which carries over as uncertainty on the following results from a quantitative point of view. We now turn to the dynamical response of the molecule. We first consider the optical response of N_2 in Fig. 1(a). In the lower-energy region below and near emission threshold (IP = 15.1 eV), we see a much fragmented spectrum, typical for covalent molecules. At higher energies, it turns into a smooth and considerably spread continuum spectrum. In Figs. 1(b)–1(d), we consider the time evolution of the dipole moment for three selected laser frequencies, that is, 24.5, 36.7, and 58.5 eV, indicated in Fig. 1(a), which deliver different characteristic behaviors. The first value lies in the upper tail of a peak in the optical response. We thus expect a resonant response. The two other values lie in regions where the optical response vanishes and we expect nonresonant dynamics. This is indeed confirmed in Figs. 1(b)–1(d). In Fig. 1(b), sizable dipole oscillations persist long after the pulse duration, typical of a resonant excitation. Figure 1(c) instead shows a standard off-resonant response: the dipole signal quickly dies off once the pulse is over. In the largest frequency case shown in Fig. 1(d), the dipole moment initially behaves as in a nonresonant case, i.e., dying out as expected. However, surprisingly, a long-lasting dipole signal reappears after $\simeq 5$ fs. Closer inspection of the evolving dipole on a logarithmic scale (not shown) reveals that the envelope of the dipole signal up to $\simeq 8$ fs increases exponentially, as is typical for an instability. In order not to be fooled by artifacts, we have scrutinized our numerical treatment by varying numerical parameters and by performing control calculations using two other full three-dimensional (3D) computer packages (EDAMAME [43] and QDD [36]); for details, see the Supplemental Material (SM) [44]. The effect persists. It is thus likely to be genuine, at least at the TDLDA level, and deserves a further analysis. We have also varied physical conditions as orientation of the molecule, ionic motion, and carrier envelope phase (CEP). The dipole instability appears only if laser polarization and symmetry axis are aligned. Ionic motion and CEP have negligible effects for the present pulse profile. For details, see the SM. In Fig. 2, we first analyze level depletions, see Eq. (1). The upper panel illustrates the time evolution of electron content for one chosen pulse frequency. Electron emission is very fast, and the electron content n_α and the depletion $\bar{n}_\alpha$ accordingly level off very quickly. The exciting aspect is that the lowest level has the largest depletion, much larger than the depletion for all the other (higher-lying) states. This comes very close

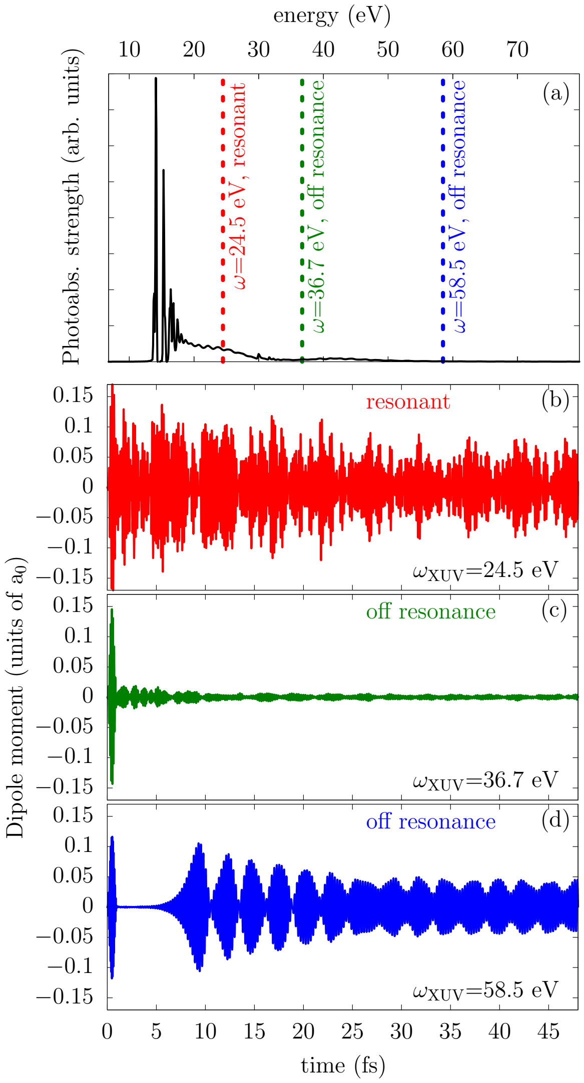

FIG. 1. (a) Photoabsorption strength of N_2 (linear scale). The vertical dashes indicate the three frequencies considered in (b), (c), and (d). (b–d) Dipole moment after an XUV excitation of duration of 1 fs, frequency ω_{XUV} as indicated, and field strength E_0 such that the total ionization is about one charge unit for each case, which is $I = 0.56 \times 10^{15}\text{W/cm}^2$ (b), $I = 1.4 \times 10^{15}\text{W/cm}^2$ (c), and $I = 7.0 \times 10^{15}\text{W/cm}^2$ (d).

to the instantaneous-hole scenario used in many theoretical investigations.

The lower panel of Fig. 2 displays the final depletions as functions of pulse frequency ω_{XUV}. At the lower frequencies, electron depletion occurs predominantly from the HOMO orbital, as expected. At the upper end, depletion approaches an equidistribution similar to observations in Na clusters and C_{60} [22–24]. But in between, we find an occupation inversion over a wide range of frequencies with, by far, the dominant depletion coming from the deepest level $2\Sigma_g$. We observed the same effect in other covalent molecules such as acetylene. Such an occupation inversion in a certain frequency range might be due to a continuum resonance enhancing the transition matrix elements selectively, but this requires a closer inspection.

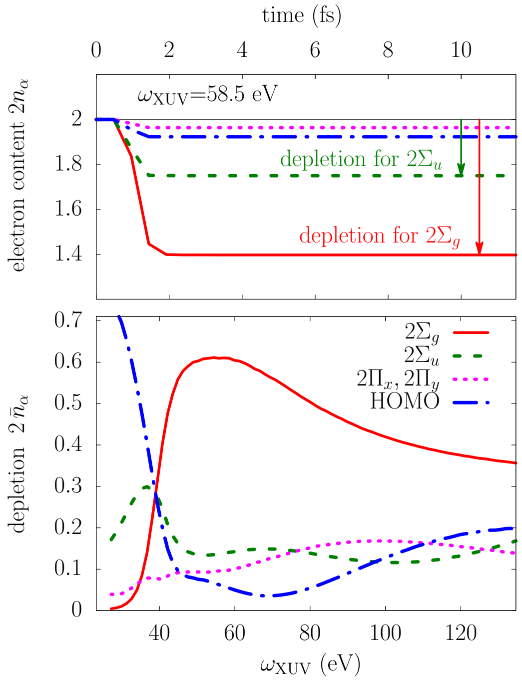

FIG. 2. (Top) Time evolution of the electron content $2n_\alpha(t)$ (factor 2 for spin degeneracy) of each s.p. state α (see legend in lower panel), after a 1-fs XUV pulse of frequency $\omega_{\text{XUV}} = 58.5$ eV. Level depletions $\bar{n}_{2\Sigma_g}$ and $\bar{n}_{2\Sigma_u}$ are indicated by vertical arrows. (Bottom) Level depletion $2\bar{n}_\alpha$ of the five initially occupied states as functions of frequency ω_{XUV}. Field strengths E_0 are adjusted to total ionizations of about 1 for each case.

The link between occupation inversion and the observed dipole instability looks striking. In a simple model with a couple of fixed electron levels coupled to the photon field, one can show that the mechanism looks the same as in a laser [45,46]. The energy reservoir contained in the occupation inversion feeds the dipole oscillations coherently. This leads to an initial exponential increase of the dipole amplitude, which turns into a steady oscillation once the reservoir is used up. For the reason of space, we will present the details in a forthcoming publication.

For the moment, there remain two ideas yet to be addressed: firstly, to propose a potential experimental observation of such an effect, and secondly, to exclude any artifact from the mean-field approach in TDLDA. Let us successively explore both aspects. Depletion and dipole moment are not directly observable by experiment. Still, a possible experimental identification of the dipole instability can be found in the PES. Figure 3 shows the PES after irradiation by a 1-fs pulse with $\omega_{\text{XUV}} = 63.9$ eV and $E_0 = 15.9\,\text{eV}/a_0$. Two different PES are plotted: one recorded in an early time window up to 10 fs (basically before the onset of the instability) and one computed at the end of the simulation time (100 fs). The early PES exhibits the standard peaks for a one-photon process with energies at $\varepsilon_\alpha + \omega_{\text{XUV}}$ (vertical dashes in Fig. 3). These peaks are very broad because the pulse is very short and because the s.p. energies move down by about 8 eV with respect to the ground state s.p. energies, due to emission and subsequent Coulomb charging [41]. The late PES consists of the early

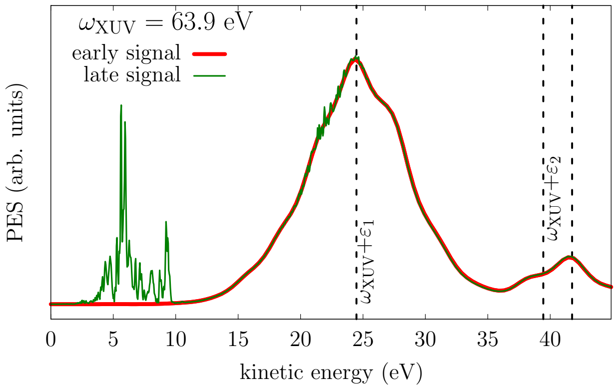

FIG. 3. Photoelectron spectra (linear scale), after a 1-fs XUV excitation with $\omega_{XUV} = 63.9$ eV, and field strength $E_0 = 15.9\,\mathrm{eV/a_0}$, computed at 10 fs (thick green line) or at 100 fs (thin black line). The faint dashed vertical lines indicate the s.p. energies shifted by the pulse frequency, see text for detail.

PES plus an additional low-energy structure, which does not fit to any combination $\varepsilon_\alpha + n\omega_{XUV}$ (with integer n). The fact that this structure shows up at later times suggests that it is a signature of the dipole instability. Indeed, the Fourier transform of the dipole moment signal at late times exhibits an oscillation frequency of $\omega_{instab} = 16.4$ eV. And the peaks at low energies might correspond to the actual s.p. energies (IP ≈ 28.6 eV) plus $2\omega_{instab}$.

Time-resolved PES measurements could thus produce unambiguous signals of the dipole instability. But achieving this remains demanding. Firstly, one needs cases with occupation inversion. Secondly, the PES from one-photon processes alone has to hit a well-separated energy gap for the structure associated with the instability to inhabit. Further theoretical investigations are needed to find more examples of promising laser setups.

Thus far, we have considered frozen ions and a pure mean-field (TDLDA) description of electrons. We checked the effect of ionic motion and it makes no difference. This is plausible in view of the extremely short time scales and ion masses. The impact of dynamical electron-electron correlations requires a closer look. To that end, we include electronic dissipation within RTA [25,36] (incoherent dynamical correlations). Figure 4 compares the time evolution of the TDLDA dipole moment to the RTA result. The pulse parameters are the same as in Fig. 3. Dissipation reduces the dipole instability but a sizable dipole oscillation remains. The result is corroborated by a simple comparison of time scales. The dipole instability increases one order of magnitude in 2 fs while the typical relaxation time for N_2 at the given excitation energy is about 5 fs. This estimate of time scales also tells us that the XUV pulses have to be shorter than the relaxation time, to let the instability live, and shorter than the instability time to disentangle dipole oscillations created by the laser pulse and those from the instability. For the ultrafast scenarios investigated here, time scales are thus forgiving and tend to validate TDLDA.

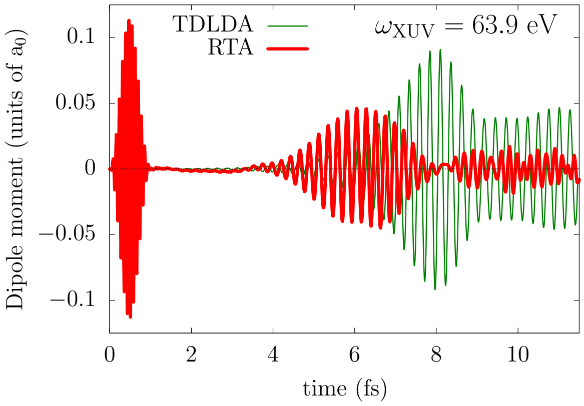

FIG. 4. Time evolution of the dipole moment computed within TDLDA or RTA. Same pulse parameters as in Fig. 3.

To conclude, we have investigated the excitation dynamics of electrons in N_2 irradiated by an ultrashort XUV pulse. It turns out that a proper choice of laser parameters allows to produce an almost perfect population inversion. Such a mechanism represents a physical realization of the instantaneous hole excitation used in numerous modelings of ultrafast processes. As a very interesting side effect, we find that the population inversion generates an unstable dynamical regime of the electron cloud, which develops spontaneously sizable dipole oscillations. We checked that the instability is not caused by numerical artifacts and that it persists even when dynamical electron correlations are included. A possible experimental signal can be found in PES and even better in time-resolved PES.

These results call for further theoretical investigations, which are underway. Preliminary results indicate that the observed instability is not specific to N_2; we found similar behaviors in acetylene and in one-dimensional model systems. We also observed dipole instabilities with longer laser pulses and/or lower intensities. The appearance of the instability results from a subtle balance between time scales (growth time of the instability, relaxation time of the dipole signal from dissipation, length of laser pulse) and off-resonance conditions (the dipole signal has to shrink sufficiently right after the pulse to render the instability visible). It requires further investigations to develop systematics. A first step in that direction is to study the instability as such by eliminating the laser and come back to the mechanism of instantaneous hole excitation, which simplifies modeling and allows to explore trends as, e.g., with excitation energy or hole states. These complementary results will be presented in forthcoming publications. For subsequent studies there remains the question of what a more elaborate theory with coherent correlations would produce in such a case. And, of course, a final clarification has to come from experiment.

This work was granted access to the HPC resources of CalMiP (Calcul en Midi-Pyrénées) under the allocation P1238, and of RRZE (Regionales Rechenzentrum Erlangen).

[1] F. Krausz and M. Ivanov, Rev. Mod. Phys. **81**, 163 (2009).

[2] F. Calegari, G. Sansone, S. Stagira, C. Vozzi, and M. Nisoli, J. Phys. B **49**, 062001 (2016).

[3] K. Ueda, E. Sokell, S. Schippers, F. Aumayr, H. Sadeghpour, J. Burgdörfer, C. Lemell, X.-M. Tong, T. Pfeifer, F. Calegari *et al.*, J. Phys. B: At. Mol. Opt. Phys. **52**, 171001 (2019).

[4] T. Jahnke, U. Hergenhahn, B. Winter, R. Dörner, U. Frühling, P. V. Demekhin, K. Gokhberg, L. S. Cederbaum, A. Ehresmann, A. Knie *et al.*, Chem. Rev. **120**, 11295 (2020).

[5] A. Marciniak, V. Despré, V. Loriot, G. Karras, M. Hervé, L. Quintard, F. Catoire, C. Joblin, E. Constant, A. Kuleff *et al.*, Nat. Commun. **10**, 337 (2019).

[6] H. J. B. Marroux, A. P. Fidler, A. Ghosh, Y. Kobayashi, K. Gokhberg, A. I. Kuleff, S. R. Leone, and D. M. Neumark, Nat. Commun. **11**, 5810 (2020).

[7] I. S. Wahyutama, T. Sato, and K. L. Ishikawa, Phys. Rev. A **99**, 063420 (2019).

[8] D. R. Austin, A. S. Johnson, F. McGrath, D. Wood, L. Miseikis, T. Siegel, P. Hawkins, A. Harvey, Z. Masin, S. Patchkovskii *et al.*, Sci. Rep. **11**, 2485 (2021).

[9] M. Ruberti, Phys. Chem. Chem. Phys. **21**, 17584 (2019).

[10] L. S. Cederbaum, W. Domcke, J. Schirmer, and W. V. Niessen, *Advances in Chemical Physics*, Vol. 65, edited by I. Prigogine and S. A. Rice (Wiley, New York, 1986), p. 115.

[11] L. Cederbaum and J. Zobeley, Chem. Phys. Lett. **307**, 205 (1999).

[12] R. Weinkauf, P. Schanen, A. Metsala, E. W. Schlag, M. Buergle, and H. Kessler, J. Phys. Chem. **100**, 18567 (1996).

[13] F. Remacle, R. D. Levine, E. W. Schlag, and R. Weinkauf, J. Phys. Chem. A **103**, 10149 (1999).

[14] F. Remacle and R. D. Levine, Proc. Natl. Acad. Sci. USA **103**, 6793 (2006).

[15] A. I. Kuleff and L. S. Cederbaum, Phys. Rev. Lett. **106**, 053001 (2011).

[16] A. I. Kuleff, N. V. Kryzhevoi, M. Pernpointner, and L. S. Cederbaum, Phys. Rev. Lett. **117**, 093002 (2016).

[17] N. V. Golubev, J. Vaníček, and A. I. Kuleff, Phys. Rev. Lett. **127**, 123001 (2021).

[18] C. E. M. Gonçalves, R. D. Levine, and F. Remacle, Phys. Chem. Chem. Phys. **23**, 12051 (2021).

[19] F. Khalili, M. Vafaee, and B. Shokri, Phys. Chem. Chem. Phys. **23**, 23005 (2021).

[20] E. Runge and E. K. U. Gross, Phys. Rev. Lett. **52**, 997 (1984).

[21] S. Goedecker, M. Teter, and J. Hutter, Phys. Rev. B **54**, 1703 (1996).

[22] S. Vidal, Z. P. Wang, P. M. Dinh, P.-G. Reinhard, and E. Suraud, J. Phys. B: At. Mol. Opt. Phys. **43**, 165102 (2010).

[23] P. M. Dinh, S. Vidal, P.-G. Reinhard, and E. Suraud, New J. Phys. **14**, 063015 (2012).

[24] C.-Z. Gao, P. Wopperer, P. M. Dinh, E. Suraud, and P.-G. Reinhard, J. Phys. B: At. Mol. Opt. Phys. **48**, 105102 (2015).

[25] P.-G. Reinhard and E. Suraud, Ann. Phys. **354**, 183 (2015).

[26] R. M. Dreizler and E. K. U. Gross, *Density Functional Theory: An Approach to the Quantum Many-Body Problem* (Springer-Verlag, Berlin, 1990).

[27] J. P. Perdew and Y. Wang, Phys. Rev. B **45**, 13244 (1992).

[28] J. P. Perdew and A. Zunger, Phys. Rev. B **23**, 5048 (1981).

[29] E. Fermi and E. Amaldi, Accad. Ital. Rome **6**, 117 (1934).

[30] C. Legrand, E. Suraud, and P.-G. Reinhard, J. Phys. B: At. Mol. Opt. Phys. **35**, 1115 (2002).

[31] P. Klüpfel, P. M. Dinh, P.-G. Reinhard, and E. Suraud, Phys. Rev. A **88**, 052501 (2013).

[32] P.-G. Reinhard and E. Suraud, Theoret. Chem. Acc. **140**, 63 (2021).

[33] C. A. Ullrich, J. Mol. Struct. (THEOCHEM) **501-502**, 315 (2000).

[34] P.-G. Reinhard, P. D. Stevenson, D. Almehed, J. A. Maruhn, and M. R. Strayer, Phys. Rev. E **73**, 036709 (2006).

[35] P. M. Dinh, L. Lacombe, P.-G. Reinhard, E. Suraud, and M. Vincendon, Eur. Phys. J. B **91**, 246 (2018).

[36] P. M. Dinh, M. Vincendon, F. Coppens, E. Suraud, and P.-G. Reinhard, Comput. Phys. Commun. **270**, 108155 (2022).

[37] F. Calvayrac, P.-G. Reinhard, E. Suraud, and C. A. Ullrich, Phys. Rep. **337**, 493 (2000).

[38] F. Calvayrac, P.-G. Reinhard, and E. Suraud, Ann. Phys. **255**, 125 (1997).

[39] A. Pohl, P.-G. Reinhard, and E. Suraud, Phys. Rev. Lett. **84**, 5090 (2000).

[40] A. Pohl, P.-G. Reinhard, and E. Suraud, J. Phys. B: At. Mol. Opt. Phys. **34**, 4969 (2001).

[41] P. Wopperer, P. M. Dinh, P.-G. Reinhard, and E. Suraud, Phys. Rep. **562**, 1 (2015).

[42] P. M. Dinh, P. Romaniello, P.-G. Reinhard, and E. Suraud, Phys. Rev. A **87**, 032514 (2013).

[43] D. Dundas, J. Chem. Phys. **136**, 194303 (2012).

[44] See Supplemental Material at http://link.aps.org/supplemental/10.1103/PhysRevA.107.L020801 for more details on numerical aspects and the impact of ionic motion, orientation of the molecule relative to the photon pulse, and carrier envelope phase.

[45] H. Haken, *Laser Theory* (Springer, Berlin, 1983).

[46] H. Haken, *Introduction to Laser Physics* (Springer, Berlin, 1991).